Evidence for the presence of Mn(III) intermediates in the bacterial oxidation of Mn(II)

Samuel M. Webb*, Gregory J. Dick†, John R. Bargar*, and Bradley M. Tebo†‡

*Stanford Synchrotron Radiation Laboratory, Menlo Park, CA 94025; and †Scripps Institution of Oceanography, La Jolla, CA 92093-0202

Bacterial oxidation of Mn(II) to Mn(IV) is believed to drive the oxidative segment of the global biogeochemical Mn cycle and regulates the concentration of dissolved Mn(II) in the oceanic water column, where it is a critical nutrient for planktonic primary productivity. Mn(II) oxidizing activity is expressed by numerous phylogenetically diverse bacteria and fungi, suggesting that it plays a fundamental and ubiquitous role in the environment. This important redox system is believed to be driven by an enzyme or enzyme complex involving a multicopper oxidase, although the biochemical mechanism has never been conclusively demonstrated. Here, we show that Mn(II) oxidation by spores of the marine *Bacillus* sp. strain SG-1 is a result of two sequential one-step electron transfer processes, both requiring the putative multicopper oxidase, MnxG, in which Mn(III) is a transient intermediate. A kinetic model of the oxidation pathway is presented, which shows that the Mn(II) to Mn(III) step is the rate-limiting step. Thus, oxidation of Mn(II) appears to involve a unique multicopper oxidase system capable of the overall two-electron oxidation of its substrate. This enzyme system may serve as a source for environmental Mn(III), a strong oxidant and competitor for siderophore-bound Fe(III) in nutrient-limited environments. That metabolically dormant spores catalyze an important biogeochemical process intimately linked to the C, N, Fe, and S cycles requires us to rethink the role of spores in the environment.

kinetics | multicopper oxidase | spores | x-ray absorption near-edge spectroscopy

L ittle is known about the chemical mechanisms responsible for bacterially mediated Mn(II) oxidation. Mn(IV) is the thermodynamically favored oxidation state in surface waters, yet abiotic Mn(II) oxidation is slow under most environmental conditions (1). Microbial processes catalyze the oxidation of Mn(II) to Mn(IV) by up to five orders of magnitude faster than surfaced catalyzed reactions (2–4), and most Mn oxides found in soil, sediments, and aquatic environments are thus believed to be of biogenic origin (2, 3, 5). Mn(II) oxidation catalysis has been observed in diverse groups of bacteria and fungi (4, 6). Some of the best examples of Mn(II) oxidizers as model organisms include the bacteria *Leptothrix discophora* (7), *Pseudomonas putida* (8), and spores of marine *Bacillus* sp. strain SG-1 (9). By understanding the detailed enzymatic mechanisms of Mn(II) oxidation and Mn(IV) oxide formation, we can gain further insight into the roles of these processes in the environment and how they tie into the global cycling of toxic and nutrient metals and organic carbon.

Previous work has identified at least some of the genes involved in Mn(II) oxidation and determined that the putative proteins are related to the family of multicopper oxidases (MCOs) (6, 10, 11). This observation is enigmatic, however, because known MCOs oxidize their substrates by one electron, whereas oxidation of Mn(II) to Mn(IV) requires the transfer of two electrons. This putative biochemical mechanism for bacterial oxidation of Mn(II) has never been conclusively demonstrated. Because all MCOs known to date oxidize their substrate through a one-electron process, if structure function relationships of MCOs hold true in the case of the Mn(II) oxidases, then

we should expect that Mn(II) would be oxidized to Mn(III). Bargar and colleagues (12, 13) have shown that a solid-phase Mn(III) oxide is not produced during oxidation by *Bacillus* sp. strain SG-1. Thus, questions arise as to whether Mn(II) is oxidized in a two-step fashion, progressing through a transient, complexed Mn(III) intermediate, or whether the Mn oxidase has a unique two-electron transfer activity for a MCO. Three general pathways can be proposed in which Mn(II) oxidation might proceed after binding of Mn(II) to the enzyme: (*i*) The oxidation could proceed through a direct two-electron, one-step process. In this case, no Mn(III) intermediates would be present. This process, however, is thought to be unlikely, because the two electrons removed from Mn(II) are not energetically equivalent (14, 15). (*ii*) The Mn oxidizing factor could oxidize Mn(II) to Mn(III), followed by dissociation of Mn(III) from the enzyme and rapid disproportionation of Mn(III) to Mn(II) and Mn(IV). This process is thought to be unfavorable because of the energetics involved, i.e., it would require a net input of energy to produce free Mn^{3+} (using published potentials) or would require the presence of a low potential Mn(III)-binding site (which would likely stabilize Mn(III) with respect to disproportionation). (*iii*) Mn(II) could be oxidized through two, enzymatically mediated, one-electron transfer reactions. This two-step mechanism is believed to be more favorable than the above pathways, assuming that the Mn^{3+}–enzyme complex/Mn^{2+} couple has a redox couple sufficiently lower than the published free Mn^{3+}/Mn^{2+} couple (6). Because of the analogous nature of the bacterial Mn(II)-oxidizing factor and MCOs, we hypothesize that Mn(III) intermediates should exist in the biological oxidation of Mn(II). This analogy suggests that pathways *ii* or *iii* should be the operative mechanism.

We have used trapping chemistry to test the existence of possible Mn(III) intermediates. Here, we show continuous *in situ* spectroscopic and kinetic evidence for the existence of a transient Mn(III) intermediate in the bacterial oxidation of Mn(II) by complexing Mn(III) with pyrophosphate, $P_2O_7^{4-}$ (PP). If Mn(III) intermediates are formed and the putative Mn(III)-enzyme site is relatively labile, then the Mn(III)–PP complex should be observed in solution, provided PP is present in sufficient excess. The presence of such Mn(III) in the experiment would therefore demonstrate that Mn(III) is produced during Mn(II) oxidation. Furthermore, if Mn(III)–PP complexes were shown to be consumed in the process, then one could conclude that the Mn(III) trapped represents an intermediate species. In addition, PP may stabilize abiotic reactions of Mn(II) and Mn(IV) to form Mn(III)–PP complexes. As shown below, interference from abiotic reactions can be reduced sufficiently if the excess concentration of PP is minimized.

Materials and Methods

Spectroscopic Mn(III) Trapping Experiments. Mn(III) and its hydrolysis products have short lifetimes (seconds) in aqueous solution

---

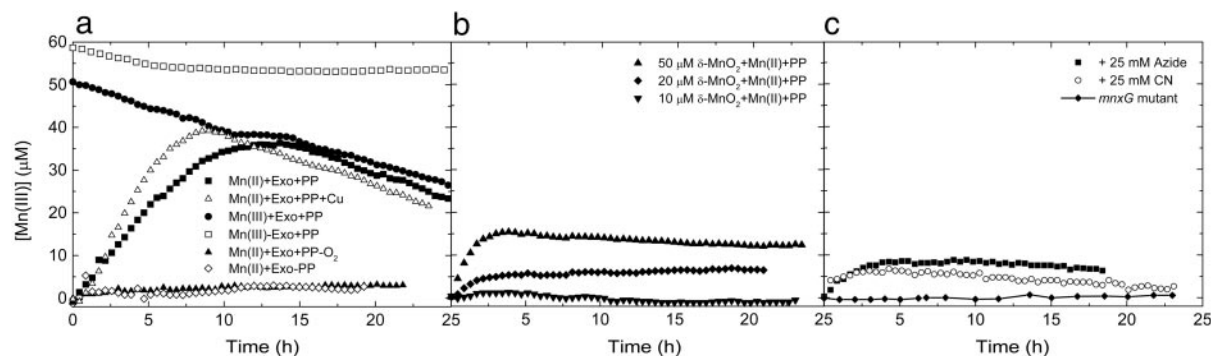**Fig. 1.** Measurements of Mn(III)–PP complexes under various experimental conditions. (*a*) Control experiments are given by ◇ (no PP present) and ▲ (no oxygen present). In these conditions, little Mn(III)–PP signal is observed and is attributed to drift of the spectrometer. The Mn(III)–PP complex is stable, as shown by the data indicated by □. Production and decay of Mn(III)–PP complexes in systems with exosporium plus Mn(II) is shown by ■. The decay of Mn(III) by the exosporium can also be achieved by direct addition of Mn(III) to the exosporium suspension, as indicated by ●. The effect of addition of 50 nM CuCl$_2$ is shown by △. (*b*) Measurements of Mn(III)–PP produced by the abiotic reactions of Mn(II) and Mn(IV) as a function of Mn(IV) concentration. [δ-MnO$_2$] = 50 μM (▲), [δ-MnO$_2$] = 20 μM (◆), [δ-MnO$_2$] = 10 μM (▼). (*c*) Measurements of the inhibition of Mn(III)–PP formation in the presence of metallo-enzyme inhibitors such as sodium azide (■) and sodium cyanide (○). Measurements performed with exosporium derived from spores with transposon insertions into the *mnxG* gene show no production of Mn(III) (◆). All measurements are performed with 0.5 mM PP and 20 mM Hepes, pH ≈7.6.

as a result of rapid disproportionation. However, Mn(III) may be stabilized through ligand-binding complexes. Chemical trapping experiments were designed to scavenge and complex any Mn(III) that may be produced in the biogenic oxidation of Mn(II). PP was chosen as a complexing ligand for this study because it forms a strong, stable complex with Mn(III) (log $k_{apparent}$ = 31.35 at pH ≈ 8) (16) and the complex is strongly colored in UV-visible region (λ_1 = 480 nm, ε_1 = 65 M^{-1}; λ_2 = 258 nm, ε_2 = 6,750 M^{-1}).

Experiments were carried out by monitoring the UV-visible absorbance spectra of the samples as a function of reaction time with an Ocean Optics (Dunedin, FL) fiber-optic dip probe spectrometer to provide continuous, *in situ* monitoring of the absorbance in small solution volumes. Cultures of *Bacillus* sp. SG-1 were grown in a seawater media containing yeast extract and peptone until sporulation occurred (17), and the spores were cleaned to remove vegetative cell debris. Mn oxides formed during the growth process were cleaned from the spores by using Tris-buffered (pH 7.5) solutions containing EDTA and ascorbic acid in a series of rinse/centrifugation steps as described in ref. 18. The exosporium, which provides the Mn-oxidizing factor (19), was isolated and concentrated by processing the cleaned spore suspensions through a French press, followed by centrifugation. All experiments were carried out at pH ≈ 7.6, buffered with 20 mM Hepes. PP, when used as a trapping ligand, was used at a concentration of 0.5 mM and was determined to be free of Fe contamination. SG-1 exosporium was added as the concentrated extract in 100-μl aliquots to a total experimental solution volume of 5 ml. Experiments were initiated by adding MnCl$_2$ at concentrations from 25 to 150 μM. Abiotic control experiments were carried out by using poorly crystalline δ-MnO$_2$ (20) as a model Mn(IV) phase. δ-MnO$_2$ was chosen because x-ray absorption near-edge spectroscopy (XANES) and extended x-ray absorption fine structure evidence suggests that it is most similar to the primary biological product of Mn(II) oxidation (12, 13).

Nonoxidizing SG-1 Mutants. A nonoxidizing transposon mutant of *Bacillus* sp. strain SG-1, LTM18, as described by van Waasbergen *et al.* (21), was used in this study. LTM18 contains a transposon insertion in the *mnxG* chromosomal region, which is believed to encode the manganese oxidase, a putative MCO (10, 19). The mutant does not produce any detectable Mn(IV) oxides when grown either on plates or in liquid media.

***μ*-XANES Spectroscopy of Mn(II) Oxidation by Whole Spores.** Biogenic Mn oxide samples to be measured with x-ray spectroscopy were

prepared with whole spores as a complement to the exosporium experiments. The incubations were begun by adding 100 μM MnCl$_2$ to a *Bacillus* sp. SG-1 spore suspension in 50 mM NaCl and 10 mM Hepes buffer, pH ≈7.8. The suspension was allowed to react for 30 min at room temperature while gently agitated.

XANES spectra were measured at the Advanced Light Source beam line 10.3.2 (22). Samples were pipetted into a cryogenic sample cell shimmed to obtain a nominal 8.5-μm thickness and frozen to a temperature of −31°C to minimize beam damage. A beam spot size of 5 × 5 μm was used to average over interstitial water and spores in small volumes (nominal volume ≈ 200 μm^3). Fluorescence spectra were recorded by using a seven-element Ge detector array. Each XANES scan required ≈8 min to complete. Multiple scan exposure tests of SG-1 biooxides showed that beam damage caused an increase in Mn(II) and damaged the biooxide structure but did not produce any detectable Mn(III).

Spectra were background-subtracted, normalized, and analyzed in SIXPACK/IFEFFIT (23, 24). Self-absorption effects were not present because the path length through the sample (8 μm) is less than its absorption length (≈15–35 μm). Least-square fitting results contained the following 1-σ error estimates: 1.7% for Mn(II), 2.6% for Mn(III), and 2.9% for Mn(IV) (12, 13).

Results and Discussion

Spectroscopic Mn(III) Trapping Experiments. The trapping experiments performed with exosporium extracts showed the formation of a Mn(III)–PP complex (Fig. 1*a*), indicating that labile Mn(III) is produced by the reaction of Mn(II) with exosporium. A range of PP concentrations (0.2–6 mM) were tested and showed that the PP concentration did not significantly affect the initial rate of Mn(III)–PP production (data not shown), suggesting that the PP concentration did not influence the production of Mn(III). As time progresses, the Mn(III)–PP complex decays (after 13–15 h in these experiments). Abiotic controls without exosporium show that the Mn(III)–PP complex is stable over this time period (Fig. 1*a*); therefore, the decay of Mn(III) from the system cannot be attributed to disproportionation of the Mn(III)–PP complex. Thus, there must be an enzymatic step of Mn(III) to Mn(IV) that acts as a reaction loss term for Mn(III), strongly implying that Mn(III) is a true intermediate. Although PP strongly binds Mn(III), some Mn(III) should remain bound to the active enzyme in the exosporium because the Mn(III)-PP and Mn(III)–enzyme complexes must be in equilibrium. Thus, PP acts as a nonreactive solution reservoir for Mn(III), which

slows the net oxidation rate, allowing the intermediate to be observed indirectly. To test this hypothesis, an extract of exosporium was added to a solution of preformed Mn(III)–PP complex: the exosporium did indeed oxidize Mn(III)–PP complexes to Mn(IV) (Fig. 1a). Additionally, the Mn(III)–PP complex was also observed to decrease at a rate similar to that in the Mn(II)-initiated experiments.

Several additional control trapping experiments (no O₂, no PP, no exosporium, and Mn(IV) additions without exosporium) were performed to ensure that the detection of Mn(III) in the experiments would not result from Mn(III) complexes created by abiotic processes or other nonrelated biogenic processes (Fig. 1 a and b).

No O₂ control. A trapping experiment was performed in the absence of oxygen in a 4% H₂/96% N₂/O₂ < 1 ppm atmosphere. Under these anoxic conditions, the exosporium was unable to oxidize Mn(II). No visible oxides or Mn(III) were produced in the reaction.

No PP control. Experiments conducted without the addition of PP to the system showed a negligible increase in the absorbance at 258 nm. This result shows that any increase in the intensity of the 258 nm line is due to Mn(III)–PP formation and not due to the leaching or production of a biological product.

No exosporium control. Mn(II) in the presence of PP and without the addition of exosporium extracts shows a slight increase in the Mn(III)–PP complex, forming at most 8 μM in 24 h (data not shown). This increase is due to the PP ligand stabilizing the Mn(III) oxidation state over Mn(II). This background production of Mn(III) is significantly less than the biogenic production of Mn(III) in nearly all experiments.

Mn(II)–Mn(IV) conproportionation. When Mn(II) and δ-MnO₂ were added to solutions containing PP, the Mn(III)–PP complex was also detected (Fig. 1b). This interaction is due to the conproportionation reaction of Mn(II) and Mn(IV) to form Mn(III), once again stabilized by the PP. This reaction becomes important only as large concentrations of MnO₂ build up in the system. A 10 μM δ-MnO₂ addition (equivalent to 10% of the total Mn in the trapping experiments) produces minimal Mn(III)–PP over the blank, whereas a 50 μM addition produces detectable Mn(III)–PP but still well below those concentrations in the biologic experiments over the same time scale. To account for the observed Mn(III)–PP in the biogenic experiments in solely an abiotic conproportionation reaction scheme, nearly all of the Mn(II) would need to have been oxidized to Mn(IV) in the first hour, which is not observed.

Exosporium extracted from mutant spores was examined to look at the dependence of the Mn(III) intermediate on the gene *mnxG*, believed to encode the Mn oxidase, that shows strong homology with MCOs (6). Trapping experiments performed with the exosporium from the mutant did not reveal the production of any measurable Mn(III) (Fig. 1c), and no solid-phase oxides were observed. Additionally, when Mn(III) was added to mutant exosporium suspensions, no decay of the Mn(III) was observed as was the case for the wild type (data not shown). This result shows that the MnxG protein is required for the oxidation of Mn(II) to Mn(III) and Mn(III) to Mn(IV). The result also further shows that the observed production of Mn(III) in the wild-type exosporium requires MnxG, the putative oxidase, and is not due to other factors in the exosporium or abiotic processes.

Several compounds have been shown to inhibit bacterial Mn(II) oxidation, such as azide and cyanide (25). These compounds are metalloprotein inhibitors and are thought to competitively bind to the active copper sites where dioxygen binds to the enzyme, thus shutting down the reaction (26). Trapping experiments were repeated in the presence of azide (25 mM) and cyanide (25 mM) to observe its effect on the production of Mn(III) (Fig. 1c). As in the case for the anoxic experiments, no visible Mn oxides were detected. The additions of these com-

pounds dramatically decreased production of Mn(III), with results again similar to that of the anoxic and blank experiments. These results are consistent with Mn oxidation (and the MnxG protein) having metalloenzyme activity similar to that of MCOs.

Mn(II) oxidation was also monitored with the addition of Cu(II). Cu could increase the reaction rate because of its requirement as a cofactor in the putative MCO protein responsible for Mn(II) oxidation. Consistent with this hypothesis, the rate of production of Mn(III) is accelerated by addition of Cu(II) (Fig. 1a).

μ-XANES Evidence for Mn(III). μ-XANES was performed to directly observe the Mn(III) species. Previous bulk XANES (12, 13) and extended x-ray absorption fine structure (13, 27) studies of Mn(II) oxidation by *Bacillus* sp. SG-1 have shown that the solid-phase product initially is a phyllomanganate similar to hexagonal or triclinic birnessite; intermediates above the detection limits of the technique (≈3% of total Mn; ref. 13) were not observed. Microscale (5-μm spot) K-edge XANES measurements of cell clumps incubated in Mn(II) were performed to spatially resolve areas of the sample where Mn(III) may be locally abundant. Principal component analysis was performed on the XANES spectra from all eight points by using SIXPACK (23). Spectra from clean spores [intracellular Mn(II)] and the birnessite product known to be present (12, 13) were included in the principal component analysis sample set to mathematically decouple likely component correlations between Mn(III) and the end-member products or reactants. This analysis showed that there were three significant components present in the system, as determined by use of the indicator function (23, 28, 29), and definitively shows that μ-XANES has detected a third species of Mn in the oxidation samples.

XANES spectra collected after 30 min of oxidation (compare Fig. 2) produced edge shapes that were noticeably different from those of Mn oxides observed in the aforementioned studies. Specifically, there is amplitude present at ≈6,556–6,558 eV in the μ-XANES spectra between the white line (absorbance maxima) for the Mn(II) and Mn(IV) species, which can be attributed to a Mn(III) species (12). Multiple-scan exposure tests on SG-1 biooxides as well as other previous studies (30) show that the appearance of Mn(III) should not be attributed to beam photoreduction.

Least-squares fitting of the spectra samples was performed to quantify the Mn(III) present by using the Mn(II) and birnessite end-members mentioned previously. Although a fit with only these Mn(II) and Mn(IV) components appears to fit the data reasonably well (upper dashed lines in Fig. 2), there is significant misfit around the region from 6,553 to 6,560 eV, which is the region where Mn(III) species typically exhibit their white lines. This misfit is many times larger than the 1-σ error level of the data. The Mn(III) present in the system is not believed to be a Mn(III) oxide solid (12), so the XANES spectra of the aqueous Mn(III)–PP complex was used as a Mn(III) standard. The addition of this Mn(III) component improves the quality of fit dramatically (lower dashed lines in Fig. 2) and decreases the reduced χ^2 on average by a factor of two. The results of the three-component fitting are given in Table 1. Because the actual form of Mn(III) present in the spore oxidation sample is not expected to be Mn(III)–PP, but rather a Mn(III) complex with the Mn oxidase or other complexing ligand, we would expect the XANES spectra of this Mn(III)-ligand species to be slightly different from Mn(III)–PP in its edge shape. This hypothesis is observed in the fitting results, where the total component sums consistently to ≈110%, suggesting that the amount of Mn(III) may be overestimated, likely because of lower amplitude of the white line for Mn(III)–PP as compared with the putative Mn(III)–ligand complex. When these results are combined with the principal component analysis, it suggests that there is an
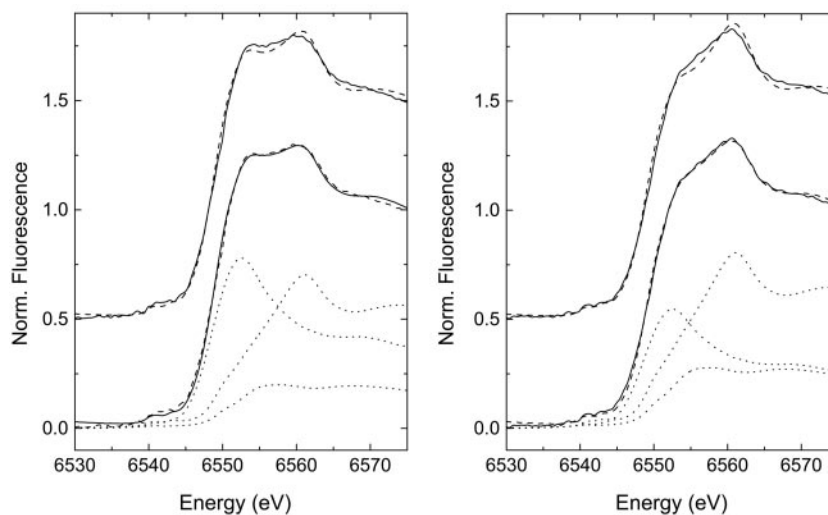
Fig. 2. Normalized spectra from μ-XANES measurements at two different points in the same sample. Data are shown by solid lines, and fits to data are shown by dashed lines. The upper dashed lines are for the two-component [Mn(II) + Mn(IV)] fits, whereas the lower ones are for the three-component [Mn(II) + Mn(III) + Mn(IV)] fits. The individual components of the three-component fits (see *Results and Discussion*) are shown in dotted lines. All measurements were performed with 10 mM Hepes, pH $\approx$7.8.

unknown Mn(III) complex present at low concentrations during the oxidation of Mn(II) by *Bacillus* sp. SG-1 when observed at the microscopic scale.

Kinetic Analysis of Mn Oxidation. The initial Mn(II) concentration added to the system was varied to obtain kinetic parameters for the production and decay of the Mn(III) intermediate. Mn(II) was added to the exosporium at different concentrations ranging from 25 to 150 μM (Fig. 3). The peak concentration of the trapped Mn(III) observed in the experiment correlates linearly with the amount of Mn(II) initially added, again showing that the observed spectroscopic product is due to the oxidation of Mn(II). The kinetics of Mn(III) formation and disappearance were modeled by using a series of equilibrium and electron transfer reactions outlined in Fig. 4. The model consists of Mn(II) binding to the enzyme site, then undergoing two individual electron transfer steps to Mn(III) and finally to Mn(IV). As illustrated, the addition of PP to the system provides a means to strip Mn(III) from the enzyme site as well as to competitively bind Mn(II). The system of differential equations that describes the model is given in Fig. 5.

The initial rates of appearance of Mn(III) (determined by first derivative plots of the Mn(III)–PP concentration) were fit by using the Lineweaver–Burk double reciprocal method to extract the K_m and v_{max} parameters (V_{init} data shown in Table 2) (31). Because the model as described consists of many highly correlated parameters, these values ($K_m = 196$ μM, $v_{max} = 24$ μM$\cdot$h^{-1}) can be used to help constrain further nonlinear fitting by linking

the forward and reverse reaction rates of the Mn(II) to Mn(III) electron transfer step. Nonlinear least-squares fitting of the data sets to the mechanistic model presented in Fig. 4 was accomplished by using software for fitting enzyme kinetics, the program DYNAFIT (32).

The optimized fit-derived parameters of the kinetic modeling are given in Table 2. The equilibrium affinity constants of the enzyme for Mn(II) and Mn(III) are expressed in relative terms to their equilibrium constants for PP because they cannot be uniquely determined in the model. There was an excellent fit of the model with the experimental data points across the entire range of initial Mn(II) concentrations (Fig. 3). The same set of kinetic parameters successfully described the trend of all of the data sets from an initial concentration of Mn(II) from 25 to 150 μM. A simpler kinetic model that did not incorporate the reversible enzyme kinetic steps was not able to describe the data (results not shown) as would be expected if it were a purely abiotic process. Inclusion of the Mn(II)/PP equilibrium reaction was also necessary to reach a single set of kinetic parameters that did not have a dependence on the initial Mn(II) concentration.
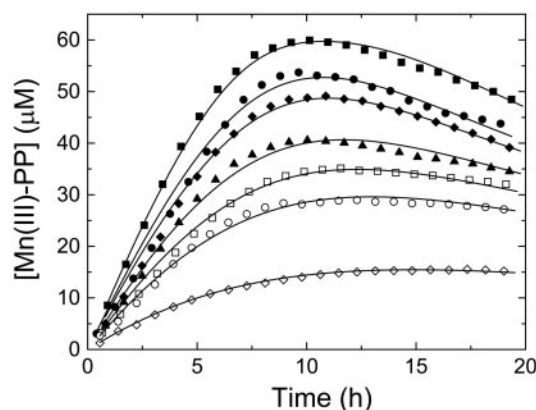
Table 1. Results from linear combination fitting of XANES spectra

Sample	Spore Mn(II), %	Mn(III)-PP, %	Birnessite Mn(IV), %
1	60	15	35
2	42	24	43
3	67	19	23
4	45	15	47
5	32	22	54
6	29	14	68
7	49	18	43
8	70	13	43

Fig. 3. Mn(III) formation as a function of initial Mn(II) concentration in the experiment. [Mn(II)]$_0$ = 150 μM (■), 100 μM (●), 90 μM (◆), 70 μM (▲), 60 μM (□), 50 μM (○), and 25 μM (◇). Solid lines to the data represent the kinetic model best fit for each concentration. All measurements were performed with 0.5 mM PP and 20 mM Hepes, pH $\approx$7.6.
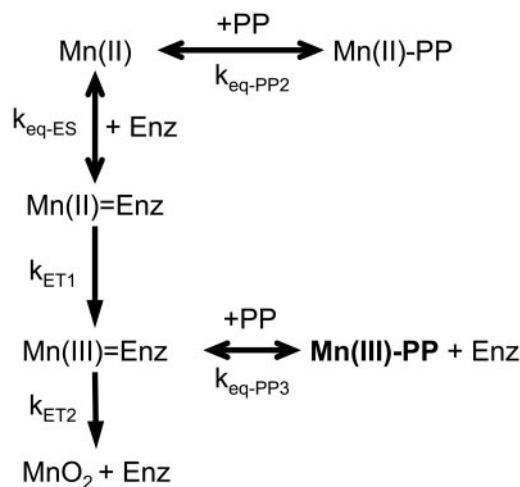
Fig. 4. Model reaction schematic for the formation and observation of Mn(III) intermediates in the oxidation of Mn(II) by *Bacillus* sp. strain SG-1.

The PP mass balance was adjusted to account for the effect of pH on the balance of protonated ligand species. In addition, the apparent rate of the electron transfer from Mn(III) to Mn(IV) is strongly correlated to the strength of the Mn(III)–PP complex relative to the enzyme complex. This conclusion can be understood from the point that if the Mn(III)–PP complex is more stable, there needs to be a more rapid reaction rate to effect the same decay rate of Mn(III). When these parameters (K_{eq-PP3} and k_{ET2}) are allowed to vary together, the relative error on the fitted values increases from ≈1% to nearly 40%. Further work by using other Mn(III) complexing agents may be of use to more accurately determine the binding affinity of the Mn(III) intermediate to the enzyme.

From these fitting results, it is evident that Mn(II) to Mn(III) is the rate-limiting step in the oxidation, because the electron transfer from Mn(III) to Mn(IV) is nearly 30 times faster. This result is not surprising, because the two electrons removed form Mn(II) are not equivalent energetically, i.e., the Mn(II) oxidation step is less energetically favorable than the Mn(III) oxidation step at near-neutral pH ($\Delta G^{\circ\prime} = 67$ kJ·mol^{-1} for Mn^{3+}/ Mn^{2+} vs. $\Delta G^{\circ\prime} = -134$ kJ·mol^{-1} for MnO$_2$/Mn^{3+}). It is important to note that the kinetic parameter K_m and fitted reaction rates are likely to be influenced by the presence of PP in the system. PP complexes Mn(II) and, therefore, the determined K_m is an apparent K_m. If the kinetic parameters are determined by using the amount of uncomplexed Mn^{2+} in solution as determined from the modeling instead of the total Mn present in the system, a much lower K_m and v_{max} ($K_m = 16$ μM, $v_{max} = 11$ μM·h^{-1}) is found. This value of K_m for Mn^{2+} is close to that determined for whole spores of *Bacillus* sp. strain SG-1 (2–5 μM, K. J. Murray and B.M.T., unpublished data) and for that of *Leptothrix discophora* ($K_m = 7$–13 μM; refs. 33 and 34). The reaction rates are expected to be much faster in the absence of PP, consistent with the overall observed reaction rates (12).

Conclusions

Both the spectroscopic and kinetic results demonstrate that a Mn(III) intermediate occurs in the oxidation of Mn(II) by *Bacillus* sp. strain SG-1 spores, which in turn implies that bacterial Mn(II) oxidation occurs as a sequence of two enzymatically mediated one-electron transfer reactions. The nature of the enzyme-Mn(III) intermediate and how the MCO is catalyzing both oxidation steps is still unknown. Further work is required to characterize the intermediate and the active oxidase(s) involved. Although the mechanism observed in this study is derived from the study of the spores of *Bacillus* sp. strain SG-1, it is likely that the production of Mn(III) intermediates in the biological production of Mn(IV) is widespread. Many other Mn(II) oxidizing bacteria have been shown to possess genes homologous to *mnxG* by encoding what appear to be similar putative multicopper Mn oxidases (6). Thus, it is likely that the Mn(II) oxidation mechanism in these other organisms will also proceed along similar lines, producing a enzyme-bound Mn(III) intermediate.

$$\frac{\partial[Mn(II)]}{\partial t} = -k_{ESf}[Mn(II)][E] + k_{ESr}[Mn(II)\cdot E] - k_{Mn2PPf}[Mn(II)][PP] + k_{Mn2PPr}[Mn(II)\cdot PP]$$

$$\frac{\partial[E]}{\partial t} = -k_{ESf}[Mn(II)][E] + k_{ESr}[Mn(II)\cdot E] + k_{Mn3PPf}[PP][Mn(III)\cdot E]$$
$$\qquad - k_{Mn3PPr}[Mn(III)\cdot PP] + k_{ET2}[Mn(III)\cdot E]$$

$$\frac{\partial[Mn(II)\cdot E]}{\partial t} = k_{ESf}[Mn(II)][E] - k_{ESr}[Mn(II)\cdot E] - k_{ET1}[Mn(II)\cdot E]$$

$$\frac{\partial[Mn(III)\cdot E]}{\partial t} = k_{ET1}[Mn(II)\cdot E] - k_{Mn3PPf}[PP][Mn(III)\cdot E] + k_{Mn3PPr}[Mn(III)\cdot PP] - k_{ET2}[Mn(III)\cdot E]$$

$$\frac{\partial[Mn(IV)]}{\partial t} = k_{ET2}[Mn(III)\cdot E]$$

$$\frac{\partial[Mn(II)\cdot PP]}{\partial t} = k_{Mn2PPf}[Mn(II)][PP] - k_{Mn2PPr}[Mn(II)\cdot PP]$$

$$\frac{\partial[Mn(III)\cdot PP]}{\partial t} = k_{Mn3PPf}[PP][Mn(III)\cdot E] - k_{Mn3PPr}[Mn(III)\cdot PP]$$

$$\frac{\partial[PP]}{\partial t} = -k_{Mn2PPf}[Mn(II)][PP] + k_{Mn2PPr}[Mn(II)\cdot PP] - k_{Mn3PPf}[PP][Mn(III)\cdot E]$$
$$\qquad + k_{Mn3PPr}[Mn(III)\cdot PP] - k_{PPprot}[PP] + k_{PPdeprot}[HPP]$$

$$\frac{\partial[HPP]}{\partial t} = k_{PPprot}[PP] - k_{PPdeprot}[HPP]$$

Fig. 5. System of differential equations describing the reaction scheme.

Table 2. List of kinetic parameters obtained from trapping experiments

$[Mn(II)]_0$, μM	V_{init}, μM·h^{-1}	K_{ET1}, h^{-1}	K_{ET2}, h^{-1}	K_{eq-ES}:K_{eq-PP2}	K_{eq-PP3}	R factor
24.86 ± 0.03	2.8 ± 0.7	18.7 ± 0.1*	573 ± 3*	74 ± 3*	380 ± 9*	0.04
49.3 ± 0.1	5.1 ± 0.6					0.55
59.1 ± 0.1	6.0 ± 0.5					0.71
70.7 ± 0.2	6.9 ± 0.6					1.29
90.2 ± 0.3	8.0 ± 0.5					1.14
103.5 ± 0.5	8.5 ± 0.7					1.73
146.3 ± 0.5	10.2 ± 0.5					0.72

V_{init} is the initial rate of Mn(III)–PP production for each of the experiments. *, kinetic parameters were the same for all Mn(II) concentrations.

That Mn(II) oxidation may lead to the formation of Mn(III) has important environmental implications. Mn(III) is a strong oxidant, present in the photosystem II oxidation of water to oxygen (35) and implicated in the degradation of lignin by fungi (36–39) and the oxidation of sulfur and nitrogen compounds (40–43). The trapping studies also show that the enzyme-bound Mn(III) is labile with respect to other ligands. Thus, Mn(III) organic complexes produced by bacteria in zones of Mn(II) oxidation may prove to be an important source of this powerful oxidant in many aquatic and terrestrial settings. Mn(III) has also been shown to compete with Fe(III) for complexation by siderophores (16). Speculation has been raised that the production of Mn(III) and the subsequent competition for siderophores may, under Fe-limiting conditions, help a bacterium acquire Fe from a stable complex that it could not use otherwise (4). Mn oxidation and the production of Mn(III) may play an important and previously unrecognized role in determining Fe bioavail-ability, which directly impacts primary productivity in the oceans and the global biogeochemical cycling of major elements, such as C, N, and S. The ability for spores to oxidize Mn(II) is a common feature of diverse species of *Bacillus* (18), suggesting that bacterial spores are not merely dormant resting stages but are important agents of coupled biogeochemical processes.

1. Morgan, J. J. (2005) *Geochim. Cosmochim. Acta* **69,** 35–48.
2. Nealson, K. H., Tebo, B. M. & Rosson, R. A. (1988) *Adv. Appl. Microbiol.* **33,** 279–318.
3. Tebo, B. M. (1991) *Deep-Sea Res.* **38,** S883–S905.
4. Tebo, B. M., Bargar, J. R., Clement, B. G., Dick, G. J., Murray, K. J., Parker, D., Verity, R. & Webb, S. M. (2004) *Annu. Rev. Earth Planet. Sci.* **32,** 287–328.
5. Wehrli, B., Friedl, G. & Manceau, A. (1995) in *Aquatic Chemistry: Interfacial and Interspecies Processes*, ed. Morgan, J. J. (Am. Chem. Soc., Washington, D.C.).
6. Tebo, B. M., Ghiorse, W. C., Waasbergen, L. G. v., Siering, P. L. & Caspi, R. (1997) in *Geomicrobiology: Interactions Between Microbes and Minerals*, eds. Nealson, K. H. & Banfield, J. F. (Miner. Soc. Am., Washington, D.C.), Vol. 35, pp. 225–266.
7. Ghiorse, W. C. (1984) *Annu. Rev. Microbiol.* **38,** 515–550.
8. Schweisfurth, R. (1973) *Z. Allg. Mikrobiol.* **13,** 341–347.
9. Nealson, K. H. & Ford, J. (1980) *Geomicrobiol. J.* **2,** 21–37.
10. van Waasbergen, L. G., Hildebrand, M. & Tebo, B. M. (1996) *J. Bacteriol.* **178,** 3517–3530.
11. Brouwers, G. J., Vijgenboom, E., Corstjens, P. L. A. M., de Vrind, J. P. M. & de Vrind-de Jong, E. W. (2000) *Geomicrobiol. J.* **17,** 1–24.
12. Bargar, J. R., Tebo, B. M. & Villinski, J. E. (2000) *Geochim. Cosmochim. Acta* **64,** 2777–2780.
13. Bargar, J. R., Tebo, B. M., Bergmann, U., Webb, S. M., Glatzel, P., Chiu, V. Q. & Villalobos, M. (2005) *Am. Mineral.* **90,** 143–154.
14. Ehrlich, H. L. (1996) *Chem. Geol.* **132,** 5–9.
15. Luther, G. W., III. (2005) *Geomicrobiol. J.*, in press.
16. Parker, D. L., Sposito, G. & Tebo, B. M. (2004) *Geochim. Cosmochim. Acta* **68,** 4809–4820.
17. Rosson, R. A. & Nealson, K. H. (1982) *J. Bacteriol.* **151,** 1027–1034.
18. Francis, C. A. & Tebo, B. M. (2002) *Appl. Environ. Microbiol.* **68,** 874–880.
19. Francis, C. A., Casciotti, K. L. & Tebo, B. M. (2002) *Arch. Microbiol.* **178,** 450–456.
20. Murray, J. W. (1974) *J. Colloid Interface Sci.* **46,** 357–371.
21. van Waasbergen, L. G., Hoch, J. A. & Tebo, B. M. (1993) *J. Bacteriol.* **175,** 7594–7603.
22. Marcus, M. A. (2004) *J. Synchrotron Radiat.* **11,** 239–247.
23. Webb, S. M. (2005) *Physica Scripta*, in press.
24. Newville, M. (2001) *J. Synchrotron Radiat.* **8,** 332–324.
25. de Vrind, J. P. M., de Vrind-de Jong, E. W., de Voogt, J. W. H., Westbroek, P., Boogerd, F. C. & Rosson, R. A. (1986) *Appl. Environ. Microbiol.* **52,** 1096–1100.
26. de Silva, D., Davis-Kaplan, S., Fergestad, J. & Kaplan, J. (1997) *J. Biol. Chem.* **272,** 14208–14213.
27. Webb, S. M., Tebo, B. M. & Bargar, J. R. (2005) *Am. Mineral*, in press.
28. Malinowski, E. R. (1977) *Anal. Chem.* **49,** 612–617.
29. Manceau, A., Marcus, M. A. & Tamura, N. (2002) in *Applications of Synchro-tron Radiation in Low-Temperature Geochemistry and Environmental Science*, eds. Fenter, P. A., Rivers, M. L., Sturchio, N. C. & Sutton, S. R. (Miner. Soc. Am., Washington, DC), Vol. 49, pp. 341–428.
30. Manceau, A., Marcus, M. A., Tamura, N., Proux, O., Geoffroy, N. & Lanson, B. (2004) *Geochim. Cosmochim. Acta* **68,** 2467–2483.
31. Lineweaver, H. & Burk, D. (1934) *J. Am. Chem. Soc.* **56,** 658–666.
32. Kuzmic, P. (1996) *Anal. Biochem.* **237,** 260–273.
33. Adams, L. F. & Ghiorse, W. C. (1985) *Appl. Environ. Microbiol.* **49,** 556–562.
34. Boogerd, R. C. & de Vrind, J. P. M. (1987) *J. Bacteriol.* **169,** 489–494.
35. Zouni, A., Witt, H.-T., Kern, J., Fromme, P., Kraus, N., Saenger, W. & Orth, P. (2001) *Nature* **409,** 739–743.
36. Glenn, J. K., Akileswaran, L. & Gold, M. H. (1986) *Arch. Biochem. Biophys.* **251,** 688–696.
37. Perez, J. & Jeffries, T. W. (1992) *Appl. Environ. Microbiol.* **58,** 2401–2409.
38. Hofer, C. & Schlosser, D. (1999) *FEBS Lett.* **451,** 186–190.
39. Schlosser, D. & Hofer, C. (2002) *Appl. Environ. Microbiol.* **68,** 3514–3521.
40. Kostka, J. E., Luther, G. W., III, & Nealson, K. H. (1995) *Geochim. Cosmo-chim. Acta* **59,** 885–894.
41. Luther, G. W., III, Ruppel, D. T. & Burkhard, C. (1998) in *Mineral-Water Interfacial Reactions: Kinetics and Mechanisms*, ed. Grundl, T. J. (Am. Chem. Soc., Washington, D.C.), Vol. ACS Symposium Series 715, pp. 265–280.
42. Klewicki, J. K. & Morgan, J. J. (1998) *Environ. Sci. Technol.* **32,** 2916–2922.
43. Klewicki, J. K. & Morgan, J. J. (1999) *Geochim. Cosmochim. Acta* **63,** 3017–3024.

MICROBIOLOGY